Measurements of Scattered Neutron Spectra at 90° Direction for Thin Targets of Ti, Fe, Ni, Cu, Nb, Mo and Pb by ^{252}Cf Fission Neutrons

By

Kazuo SHIN, Takashi FUKUHARA* and Tomonori HYODO

(Received June 29, 1983)

Abstract

The angular spectra of scattered neutrons were measured by using fission neutrons with various thin targets of Ti, Fe, Ni, Cu, Nb, Mo, and Pb to make an integral testing of fast-neutron differential scattering cross sections in the ENDF/B-IV and JENDL-1 files. Parallel beams of the fission neutrons were injected into the targets, and neutrons scattered at 90° in the laboratory system were measured with an NE-213 scintillator.

Monte Carlo calculations were done to analyze the experimental spectra. The data in the ENDF/B-IV and JENDL-1 files utilized in the calculations.

The following are pointed out in this work :

(1) The Fe and Pb spectra were reproduced well by the data in the ENDF/B-IV file.
(2) The Mo spectrum was reproduced by the JENDL-1 file better than the ENDF/B-IV file.
(3) The Cu spectrum was not reproduced by either the ENDF/B-IV file nor the JENDL-1 file.
(4) The calculation by the ENDF/B-IV data gave a harder spectrum for the Nb target than that of the experiment.
(5) The calculation by the ENDF/B-IV file gave a slight underestimate to th espectra at low energies for the Ti and Ni targets, compared with the experimental ones.

I. Introduction

The albedo model[1] is widely used in duct streaming calculations in the shielding design of nuclear reactors. Albedo data are fundamentally used in this model. Uncertainties in neutron differential scattering cross sections at large scattering angles give rise to large uncertainties in the albedo data, which may generate large errors in the duct streaming calculations.

Many types of the benchmark experiments[2]-[6] were made, and were compiled for integral testing of neutron cross sections and neutron transport codes. Few

---

* Dopartment of Nuclear Engineering. Present address; The Shikoku Electric Power Company Inc., Marunouchi 2-5, Takamatsu 769-91.

benchmark experiments have been carried out, however, for the purpose of testing differential scattering cross sections. A series of the neutron scattering experiments[7],[8] was carried out by thick slabs using collimated fission neutron beams. In the present work, the same geometrical configuration as in the previous work[8] was used to measure scattered neutrons at a 90° direction for the narrow beams of fission neutrons. Thin targets were used to decrease neutron multiple scatterings in the target. Hence, integrated information on the differential scattering cross sections was obtained from this experiment, because the obtained data were smeared by the source spectrum. Monte Carlo calculations by JUPITER code[9] were made using the data in the ENDF/B-IV[10] and JENDL-1[11] files. The calculated results will be compared with the experimental results, and the adequacy of the evaluated data will be tested at the 90° direction.

II. Experimental

1. Experimental Meethod

Figure 1 shows a schematic drawing of the experimental setup. A heavy concrete container with the dimensions of $3 m \times 3 m \times 3 m$ had a 30 cm diam. by 100 cm long hole, from which a three stepped duct (15 cm diam. $\times 82.5$ cm length, 18 cm diam. $\times 22.5$ cm length, and 20 cm diam. $\times 15$ cm length) was located. A ^{252}Cf neutron source of ~ 0.7 Ci intensity was set at the center of the hole, and neutrons were guided to the room through the duct.

Targets of Ti, Fe, Ni, Cu, Nb, Mo and Pb were utilized in the experiment. They were formed to a disk shape, the dimensions of which are shown in Table I. The target was set on the neutron beam line, the normal line of the target's front
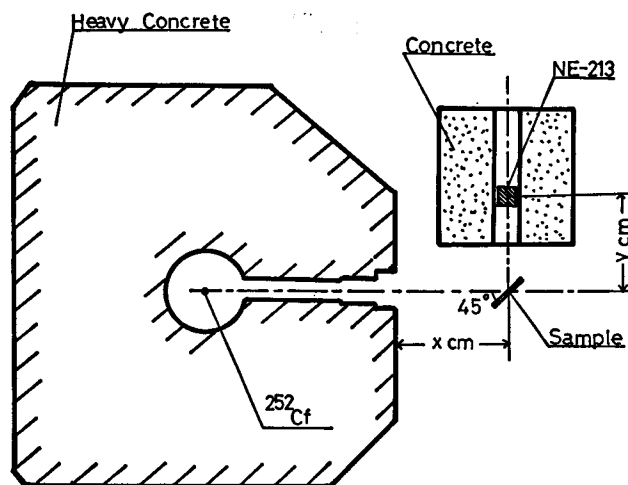

Fig. 1 Experimental arrangement.

surface being kept at 45° from the beam
line, at the position x cm from the exit of
the beam duct, where the values of x are
listed in Table I.

Scattered neutrons were detected by
a 7.5 cm diam. by 7.5 cm long NE-213
scintillator. The dectector was positioned
at y cm from the center of the target's
rear surface and at a 90° direction to the
beam line, where the values of y are
shown in Table I. The detector was
shielded from the room scattered neutrons

Table 1 Experimental Conditions

Sample	Dimensions		x (cm)	y (cm)
	Diameter (cm)	Thickness (cm)		
Ti	15	1.2	120	78
Mo	15	1.0	120	78
Ni	15	1.0	120	78
Nb	9.3	2.0	112	69.7
Ta	9.3	2.0	112	69.7
Cu	15	1.0	111.5	89.7
Pb	15	1.0	111.5	89.7
Fe	14.5	1.0	111.5	89.7

by a concrete shield having 100 cm × 100 cm × 100 cm dimensions. A heavy concrete
shield with the thickness of 60 cm was placed between the detector and the exit of
the beam duct to cut off any neutrons which came to the detector directly from the
beam duct.

Neutron pulse-height distributions were obtained from the output pulses of the
NE-213 scintillator by discriminating neutrons against gamma rays with a RHC pulse-
shape-discrimination circuit[12] and a two
dimensional multi-channel pulse-height
analyzer. The block diagram of the
measuring circuits is shown in Fig. 2.

The unfolding of the pulse-height
distributions to energy spectra was done
by the FERDO method[13] with the aid
of the response functions[14] which were
calculated by the Monte Carlo method.
The measured energy of neutrons was
from 1.5 MeV to 10 MeV.
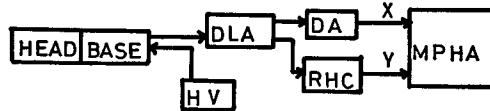
The background run was carried
out by removing the target.

HEAD : 3"×3" NE-213 Scintillator with RCA 8575
         Photomultiplier Tube
BASE : Photomultiplier Base
HV   : High Voltage Power Supply
DLA : Delay Line Amplifier
DA   : Delay Amplifier
RHC : Rise Time to Height Converter
MPHA : 2-Dimensional Multi-Channel
         Pulse-Height Analyzer

Fig. 2 Block diagram of measuring circuits.

2. Source Condition

The beam profile and the energy spectrum of the source neutron were measured
by using a 30 mCi ^{252}Cf source which was located at the center of the heavy concrete
container in place of the 0.7 Ci source. The reason is that the 0.7 Ci source was so
intense that a direct measurement of the source neutrons was difficult.

The neutron beam profile was measured at first by a 5 cm diam. by 5 cm long
NE-213, with the discrimination level being 2 MeV, at 50 cm from the duct exit by

moving the detector perpendicularly to the beam line. An ad hoc calculation method
was used to determine the beam profile, because the scintillator's diameter could not
be considered small in comparison with the diameter of the neutron beam. The
obtained result is shown in Fig. 3. The average beam radius $\bar{r}$, defined by the
following equation (1), was 13.3cm at the measured position.

$$\bar{r}=\left[\frac{1}{\pi\phi_0}\int_0^{30}\phi(r)\,2\pi r dr\right]^{1/2}, \qquad\qquad (1)$$

where ϕ_0=neutron flux on the beam line,

   r=distance from the beam center line,

and $\phi(r)$ =neutron flux at r cm from the beam center line. The radius of the neutron
beam was larger than the target radius, so the neutron flux could be considered
uniform on the target surface.

The neutron spectrum was measured on the center line of the neutron beam at
a position 50 cm from the duct exit. A proton recoil proportional counter of 5 cm
diameter filled with 4 atm. H_2 gas was used to get the normalization factor of the
spectrum for the $\sim$0.7 Ci source. The detector was set at the same position as the
NE-213, and the count rates by the two neutron sources of 30 mCi and $\sim$0.7 Ci
were measured. The source spectrum obtained by the NE-213 with the 30 mCi
source was renormalized using the ratio of the count rates given by the proportional
counter. The final result of the sources
spectrum at a position 50 cm from the
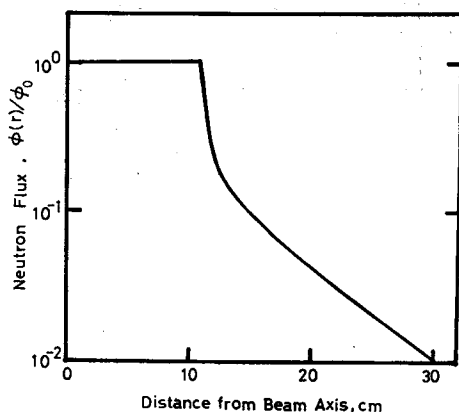duct exit is shown in Fig. 4.
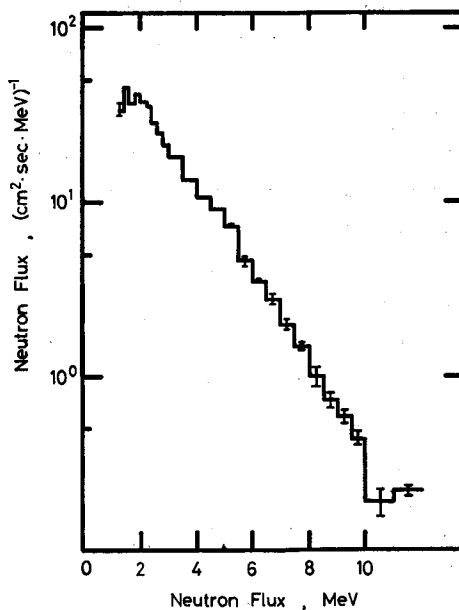

Fig. 3 Beam profile of source neutrons.

Fig. 4 Source neutron spectrum on the beam
line 50cm from beam duct exit.

III.   Error Estimation and Data Analysis

1.   Error Estimation

Errors in the measured energy spectra were caused by two reasons, the unfolding and the background. The errors due to the unfolding process were estimated by the modified FERDO code[15] on the following points : statistical uncertainty in the pulse height distributions, errors from the step function approximation and those due to the response function errors.

The background was estimated by the background run without the target. The amount of the background was rather high because the thickness of the target was thin in comparison with the neutron mean-free path. The signal to the noise ratio due to the background was about 2 in the worst case.

The gain shift of the measuring system during the experiment was checked using typical edges shown in the pulse-height distributions of gamma rays. These were generated mainly from the capture reactions of room-scattered neutrons in structual materials of the counting room. The gamma-ray pulse-height distributions were obtained simultaneously in the neutron measurements. The gain shift was shown to be negligibly small.

2.   Data Analysis

A point Monte Carlo calculation code JUPITER[9] was used to take account of the multiple scatterings of incident neutrons and the self-shielding effect of the sample to neutrons having the direction toward the detector. The calculations were carried out with the same geometry as in the experiment : The parallel beams of neutrons with the measured spectrum in Fig. 4 were injected uniformly onto the front surface of the target in the direction of 45° with respect to the normal direction of the surface. The point detector estimation method was used in the calculation of the neutron spectra. The calculation was made by the ordinary Monte Carlo method based on the pointwise cross sections of the ENDF/B-IV[10] and JENDL-1[11] files.

The error bars drawn in the calculated spectra show the estimation of the statistical uncertainty in the Monte Carlo procedure. Errors in the source spectrum, however, were ignored completely in the above error estimation. All the results of the calculation and the experiment were normalized to one incident neutron on the targets.

IV.   Result and Discussion

Fig. 5 shows the spectra at the detector point of the neutrons scattered from the Mo target. Also shown are the comparison among the measured spectrum and the calculated spectra by the ENDF/B-IV file and the JENDL-1 file. The measured
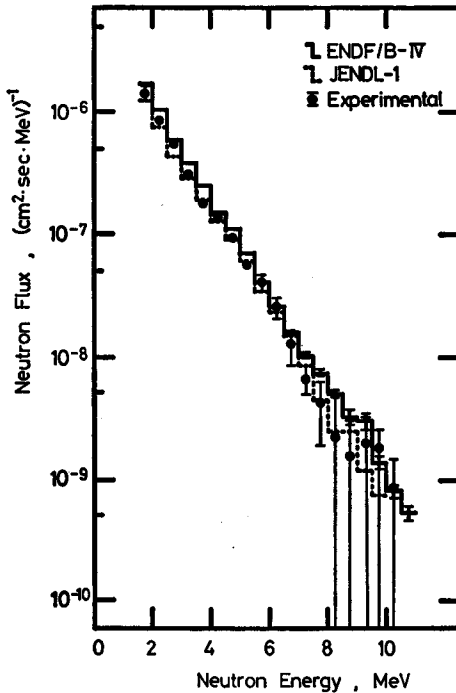
Fig. 5 Comparison of neutron spectrum at 90°
from Mo sample among the experiment
and the calculations by the ENDF/B-IV
and JENDL-1 data.

Fig. 6 Comparison of neutron spectrum at 90°
form Cu sample among the experiment
and the calculations by the ENDF/B-IV
and JENDL-1 data.

spectrum agrees fairly well with the spectrum by the JENDL-1 file, while the neutron flux by the ENDF/B-IV file is a little higher than the other two spectra.

Figure 6 shows the scattered neutron spectra from the Cu target. The measured spectrum is compared with spectra by the JENDL-1 and the ENDF/B-IV files. The follwing two points can be pointed out from this figure : 1) The flux by the JENDL-1 is higher than the ENDF/B-IV. 2) The experimental flux is higher than the calculated fluxes in the low energy region ($E_n \leq 4$ MeV).
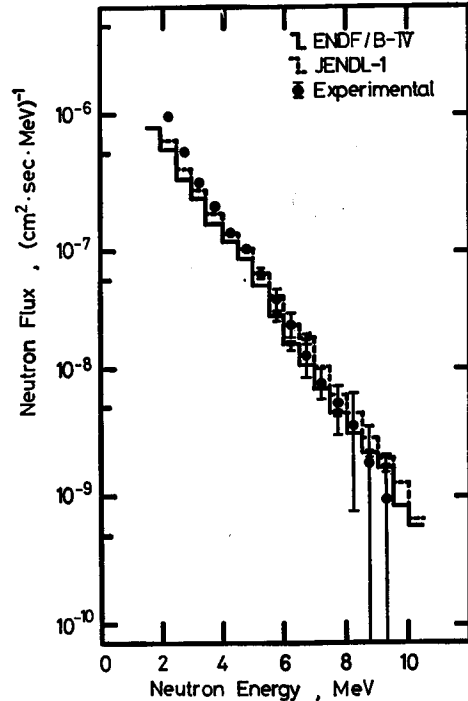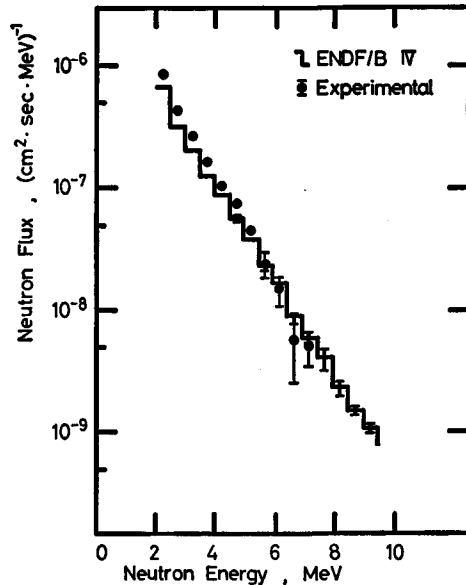
Only the ENDF/B-IV spectra will

Fig. 7 Comparison of neutron spectrum at 90° from
Fe sample between the experiment and
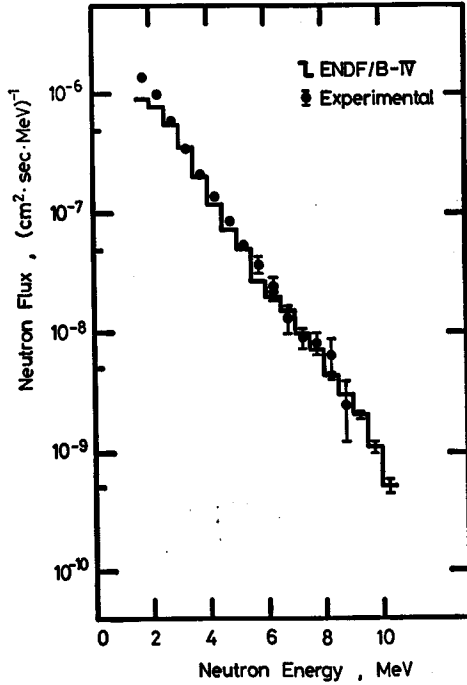the calculation by the ENDF/B-IV data.

Fig. 8 Comparison of neutron spectrum at 90° from Pb sample between the experiment and the calculation by the ENDF/B-IV data.
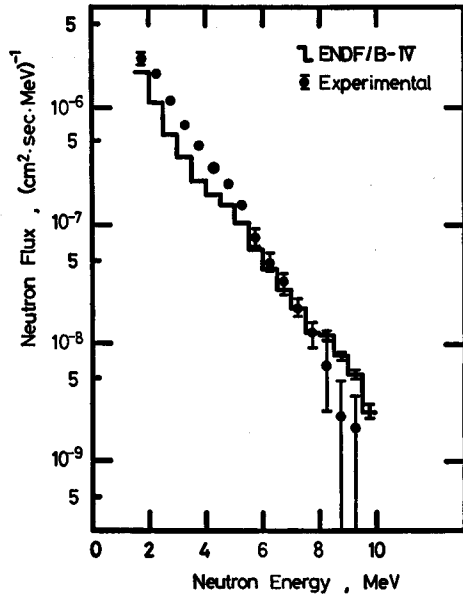

Fig. 9 Comparison of neutron spectrum at 90° from Nb sample between the experiment and the calculation by the ENDF/B-IV data.
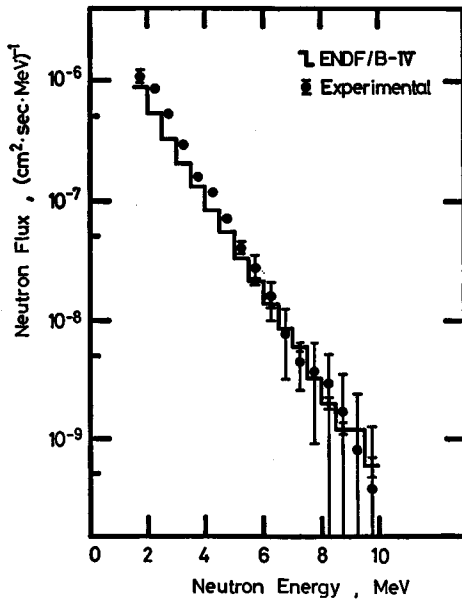

Fig. 10 Comparison of neutron spectrum at 90° from Ti sample between the experiment and the calculation by the ENDF/B-IV data.
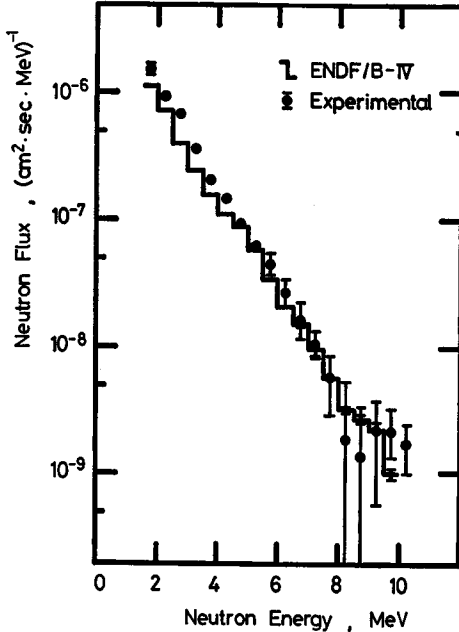

Fig. 11 Comparison of neutron spectrum at 90° from Ni sample between the experiment and the calculation by the ENDF/B-IV data.

be shown in the discussions described below for the Fe, Pb, Nb, Ti, and Ni targets.

The scattered neutron spectra from the Fe target are shown in Fig. 7. While a small difference is seen between the two spectra in the low energy region, the agreement between these spectra is fairly good on the whole. The oscillation seen in the measured spectrum near 7 MeV does not have any physical meaning, because it was caused from the saturation in the measured pulse height distribution. The data of scattering cross sections at 90° in the ENDF/B-Ⅳ file seem to be adequate in this energy range.

Figure 8 shows the neutron fluxes scattered from the Pb target. The two spectra in the figure agree very well. We can say that the evaluation by the ENDF/B-Ⅳ is adequate for the Pb scattering cross sections at a 90° direction.

Figure 9 shows the neutron spectra for the Nb target. The calculated spectrum is considerably harder than the measured spectrum.

Figure 10 shows the scattered neutron fluxes from the Ti target. A small discrepancy is seen between the measured and calculated spectra in the low energy region ($E_n \leq 5$ MeV).

Figure 11 shows the neutron spectra for the Ni target. The agreement between the measured and calculated spectra is fairly good, excluding the discrepancies seen at the low energy range ($E_n \leq 4.5$ MeV).

V. Conclusion

In this study, neutron spectra scattered from various targets were measured for the fission neutron source at the direction of 90°. The differential scattering cross sections were tested at the 90° direction by the comparison of the measured spectra with the Monte Carlo calculated spectra. The obtained results are summarized as follows :

(1)   The Fe and Pb spectra were predicted well by the data in the ENDF/B-Ⅳ file.

(2)   The Mo spectrum was reproduced by the JENDL-1 file better than by the ENDF/B-Ⅳ file.

(3)   The Cu spectrum was not reproduced by either the ENDF/B-Ⅳ file nor the JENDL-1 file.

(4)   The calculation by the ENDF/B-Ⅳ data gave a harder spectrum for the Nb target than the experiment.

(5)   The calculation by the ENDF/B-Ⅳ file gave a slight underestimate, compared with the experimental spectra at low energies for the Ti and Ni targets.

Measurements of Scattered Neutron Spectra at 90° Direction for Thin Pargets of Ti, Fe, Ni, Cu, Nb, Mo and Pb by ²⁵²Cf Fission Neutrons

25

Acknowledgement

References

1) Maerker, R. E. et al., "A Monte Carlo code Utilizing the Albedo Approach for Calculating Neutron and Capture-Gamma-Ray Distribution in Rectangular Concrete Ducts", ORNL-3964 (1967).
2) Maerker, R. E. et al, "Final Report on a Benchmark Experiment in Thick Sodium", ORNL-4880 (1974) : "Final Report on a Benchmark Experiment for Neutron Transport through Iron and Stainless Steel", ORNL-4892 (1974) ; see also, Nucl. Sci. & Eng., 52, 227 (1973).
3) Nicks, R., "The NEACRP Co-Ordinated Programme of Shielding Benchmark Experiments: Results of the First Four Single-Material Experiments in Iron", NEACRP-U-73 (1976).
4) Integral Experiments in Proceedings of the Fifth International Conference on Radiation Shielding, Ed., Roussin, R. W. et al., pp. 795-922 Knoxville (1977).
5) Tanaka, S. et al., "Shielding Benchmark Problems", JAERI-M 7843 (1978).
6) Hansen, L. F. et al, Nucl. Sci. & Eng., 35, 227 (1969) : ibid., 40, 262 (1970) : ibid., 51, 278 (1973) : ibid., 55, 345 (1974) : ibid., 60, 27 (1976) : ibid., 62, 550 (1977) : ibid., 66, 428 (1978) : ibid., 72, 35 (1979).
7) Shin, K. et al., J. Nucl. Sci. and Technol., 17, 37 (1980).
8) Shin, K. et al., Mem. of Faculty of Engineering, Kyoto Univ., 43, 331 (1981).
9) Shin, K. et al., J. Nucl. Sci. and Technol., 17, 668 (1980).
10) "ENDF/B Summary Documentation", BNL-NCS-17541 (ENDF-201), 2nd ed. (ENDF/B-IV), Garber, D., Ed., available from the National Nuclear Data Center, Brookhaven National Laboratory (Oct. 1975).
11) Igarashi, S., Nakagawa, T., Kikuchi, Y., Asami, T., and Narita, T., "Japanese Evaluated Nuclear Library Version I", JAERI-1261 (1979).
12) Furuta, Y., Kinbara, S. and Kaieda, K., Nucl. Instr. and Methods, 84, 269 (1970).
13) Burrus, W. R. and Verbinski, V. V., "Recent Developments in the Proton-Recoil Scintillation Neutron Spectrometer", ANS-SD-2, 148 (1964).
14) Shin, K., Tokumaru, H., Yoshida, M. and Hyodo, T., Memoirs of Faculty of Engineering, Kyoto Univ., 41, 116 (1979).
15) Shin, K., Uwamino, Y., and Hyodo, T., Nucl. Technol., 53, 78 (1981).